Achieving Improved Permeability by Hydrogen Bond Donor Modulation in a Series of MGAT2 Inhibitors

James S. Scott,[*a] David J. Berry,[b] Hayley S. Brown,[a] Linda Buckett,[a] David S. Clarke,[a] Kristin Goldberg,[a] Julian A. Hudson,[a] Andrew G. Leach,[a] Philip A. MacFaul,[a] Piotr Raubo,[a] & Graeme Robb.[a]

[a] AstraZeneca, Mereside, Alderley Park, Macclesfield, Cheshire, SK10 4TG, UK
[b]Durham University, School of Medicine, Pharmacy and Health, Wolfson Research Institute, Queen's Campus, Stockton on Tees, TS17 6BH, UK
Telephone: +44 (0)1625 232567. Fax: +44 (0)1625 516667
E-mail: jamie.scott@astrazeneca.com.

Keywords
Monoacylglycerol acyltransferase, MGAT2 inhibitor; metabolic syndrome; permeability; hydrogen bond donor;

Abstract
Monoacylglycerolacetyltransferase-2 (MGAT2) is a potential target for the treatment of type II diabetes. We report here the optimisation of a series of MGAT2 inhibitors with regard to their potency and permeability. Improvements in permeability, as measured by increased flux in a Caco-2 assay, were achieved through substitution at the 9-position of the core. We propose that reduction of the NH hydrogen-bond donor strength was primarily responsible for these effects.

Body text

Monoacylglycerolacetyltransferase-2 (MGAT2) is a member of the family of enzymes that catalyses the synthesis of diacylglycerol from monoacylglycerol and fatty acyl CoA.[1] It is located in the endoplasmic reticulum and is highly expressed in the small intestine.[2] Preclinical studies have shown that MGAT2 deficient mice show resistance to obesity, hyperglycaemia, hypercholesterolaemia and hepatic steatosis induced by a high fat diet.[3] Increased energy expenditure, even in the absence of a high fat diet, is at least partly responsible for these protective effects.[4] Inhibition of MGAT2 has therefore attracted interest as a potential mechanism for treatment of the metabolic syndrome. We have recently reported a novel series of MGAT2 inhibitors[5] and herein report further optimization, primarily focused on increasing the membrane permeability of the compounds.

Membrane permeability is a key consideration in drug discovery, particularly in the *in vivo* absorption of oral drugs and the ability of molecules to access intracellular targets. In general, within a chemical series, the permeability decreases with increasing polarity although other factors, such as molecular weight, are important.[6] In recent years, the strategy of keeping lipophilicity of drug candidates low has been highlighted as a way of increasing the likelihood of achieving soluble compounds that are metabolically stable and avoid potential toxicological risks.[7] One of the consequences of working in low lipophilicity space however, is that permeability is more likely to become an issue.

Systematic methylation of the three hydrogen bond donors present in our series of MGAT2 inhibitors had been previously examined.[5] This had resulted in improvements in permeability, as assessed in a Caco-2 assay (apical pH =6.5; basolateral pH = 7.4).[8] This was consistent

with a reduction in hydrogen bond donor count, but had led to an unacceptable loss in potency for the three molecular matched pairs (Figure 1). Notably, methylation of R4 appeared to have the least impact on Caco-2 permeability, with more significant changes being observed at R1 and R7. In attempts to achieve potent yet permeable compounds, we sought to retain the three donors but to modulate their strength by electronic and steric effects through substitution of the core aryl ring.[9-12]

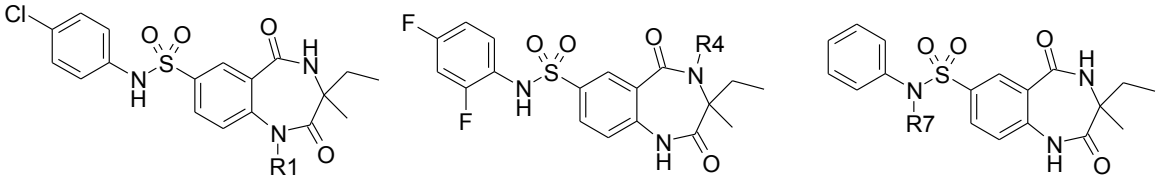

R1	H	Me
MGAT2 pIC_{50}	7.6	6.4
CACO2 A-B ($x10^{-6}$ cm/s)	5	20

R4	H	Me
MGAT2 pIC_{50}	8.0	5.1
CACO2 A-B ($x10^{-6}$ cm/s)	4	8

R7	H	Me
MGAT2 pIC_{50}	6.4	<4
CACO2 A-B ($x10^{-6}$ cm/s)	2	36

Figure 1. Effect of methylation on MGAT2 potency and permeability.

Results from aryl ring substitution of the core are shown in Table 1. In the case of fluoro subsitution (**2**-**4**), the 6-fluoro resulted in a large drop in potency whereas substitution in the 8- or 9- positions resulted in less than a two-fold change. In terms of permeability, the 6- and 8- substitutions resulted in no change, however, 9-substitution, proximal to the amide NH, did result in increased permeability. In the case of methoxy substituents (**5**-**7**), substitution at the 6-position was not tolerated with 8-substitution also resulting in a drop in potency. By contrast, 9-substitution resulted in an increase in both potency and permeability. Methyl substitution (**8**-**10**) showed similar SAR in terms of potency, with 6- and 8- substitution resulting in lower potencies relative to the un-substituted core. As before, 9-substitution resulted in increased potency and an improvement in terms of Ligand Lipophilicity Efficiency (LLE)[13] of +1.3 relative to the un-substituted core. In terms of permeability, for all three methyl isomers, the data was very similar to the un-substituted core with no improvement observed, even at the 9-position. The pyridyl analogues (**11**, **12**) were also examined. In the case of the 8-pyridyl compound the potency was lowered, however, this was accompanied by an expected drop in lipophilicity with the value for LLE remaining the same as the phenyl matched pair. Here the permeability was measured to be lower as may be expected based on a lower lipophilicity compound. The 9-pyridyl compound lost a greater degree of potency than would be expected from lipophilicity alone. Interestingly however, it showed a surprising increase in permeability relative to the isolipohilic 8-pyridyl isomer and retained similar permeability when compared to the more lipophilic aryl core. Our conclusion from these data was that modulation of the 9-position offered an opportunity to increase permeability (F, OMe, aza-N) and potency (Me, OMe) with methoxy offering an opportunity to do both simultaneously.

Table 1. Human MGAT2 potencies, lipophilicity and permeability data for core substitution.

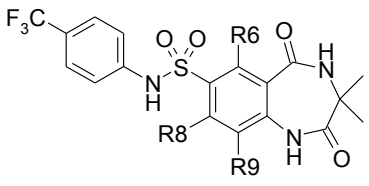

Cpd	Substitution	MGAT2 IC_{50}[a]	$logD_{7.4}$	LLE (pIC_{50}-logD)	Caco-2 A-B P_{app} ($x10^{-6}$ cm/s)
1	H	0.911	2.6	3.4	6
2	6-F	40.4	2.4	2.0	4
3	8-F	1.49	2.3	3.5	5
4	9-F	1.95	2.3	3.4	14
5	6-OMe	>100	1.9	-	7
6	8-OMe	7.61	2.8	2.3	1
7	9-OMe	0.109	2.6	4.4	12
8	6-Me	13.6	-	-	9
9	8-Me	13.4	3.0	1.9	7
10	9-Me	0.052	2.6	4.7	7
11	8-azaN	10.5	1.6	3.4	1
12	9-azaN	>66	1.8	-	10

[a] IC_{50} value from the human MGAT2 Rapidfire LCMS® assay.

Exploration of the R9 substituent (Table 2) was carried out contemporaneously in a 2,4-fluoro aniline series which had been previously shown[5] to be considerably more potent and less lipophilic than the 4-trifluoromethyl aniline (contrast matched pair **1** and **13**). Methyl substitution resulted in an increase in potency although this was less dramatic than seen previously (ΔLLE for **10** and **1** = +1.3; ΔLLE for **14** and **13** = +0.5). Cyano substitution **15** resulted in lower potency and permeability. Trifluoromethyl **16** retained potency and provided a dramatic enhancement in permeability.

Table 2. Human MGAT2 potencies, lipophilicity and permeability data for R9 substitution.

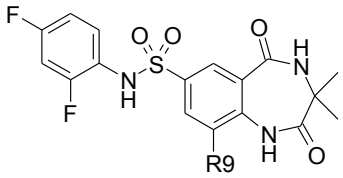

Cpd	R9 Substitution	MGAT2 IC_{50}[a]	$logD_{7.4}$	LLE (pIC_{50}-logD)	Caco-2 A-B P_{app} ($x10^{-6}$ cm/s)
13	H	0.058	1.3	5.9	5
14	Me	0.016	1.4	6.4	10
15	CN	0.405	-	-	3
16	CF_3	0.030	1.9	5.6	46

[a] IC_{50} value from the human MGAT2 Rapidfire LCMS® assay.

The effect of 9-substitution was also examined in a series with racemic methyl, ethyl (as opposed to methyl, methyl) substitution of the bis-amide ring (Table 3). Here the potency enhancements seen with 9-substitution were less marked with all substituents examined (OMe, Et, Cl) showing similar values of LLE to the un-substituted compound **17**. In terms of permeability, an enhancement was seen for all 9-substituted compounds, notably so for the chloro compound **20**. In the case of the methyl substituted compounds, these were synthesised in enantiomerically pure form based on the separation of an intermediate by chiral HPLC. Isomer **21a** (absolute stereochemistry undetermined) was approximately nine-fold more potent than enantiomeric **21b** resulting in a high value for LLE (6.5). In common with the data presented in Tables 1 and 2, methyl substitution offered little to no enhancement of permeability.

Table 3. Human MGAT2 potencies, lipophilicity and permeability data for R9 substitution.

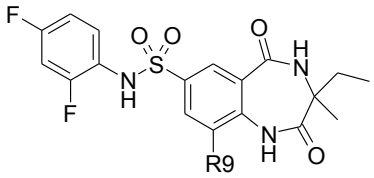

Cpd	R9 Substitution	MGAT2 IC_{50}[a]	$logD_{7.4}$	LLE (pIC_{50}-logD)	Caco-2 A-B P_{app} ($x10^{-6}$ cm/s)
17[b]	H	0.010	1.7	6.2	8
18	OMe	0.010	1.8	6.2	22
19	Et	0.004	2.1	6.3	24
20	Cl	0.009	1.9	6.1	35
21a[c]	Me	0.007	1.7	6.5	9
21b[c]	Me	0.062	1.8	5.4	14

[a]IC_{50} value from the human MGAT2 Rapidfire LCMS® assay. [b]Compound is the enantiomerically pure (*S*)-isomer. [c]Compounds are enantiomerically pure but the absolute stereochemistry is unknown

With the chloro substituent offering the largest improvements in terms of permeability,[14] this was examined in conjunction with other sulphonamide substituents (Table 4).[15] Comparison of the 2-fluoro-4-trifluoromethyl sulphonamide pair **22** and **23** with and without a 9-chloro substituent shows an approximate three-fold increase in permeability for the chloro substituted compound **23**. In the case of the 2-methoxy-4-trifluoromethyl sulphonamide **24** an increase in lipophilicity was observed together with a further increase in permeability. This compound had the highest Caco-2 value (P_{app} 58 x 10^{-6} cm/s) of any member in the series together with high potency (IC_{50} 7 nM). Interestingly, even low lipophilicity compounds containing the 2-cyano-4-methyl sulphonamide (**25**) retained reasonable Caco-2 values (>10 x 10^{-6} cm/s) despite low $logD_{7.4}$ values (~0.5). As in the case of compound **21**, a clear difference in potency between the separated enantiomers was observed.

Table 4. Human MGAT2 potencies, lipophilicity and permeability data for combinations

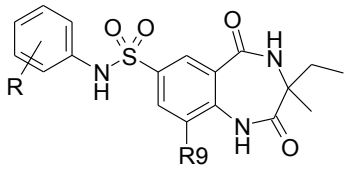

Cpd	R9 Substitution	R Aryl Substitution	MGAT2 IC_{50}[a]	$logD_{7.4}$	LLE (pIC_{50}-logD)	Caco-2 A-B P_{app} ($x10^{-6}$ cm/s)
22[b]	H	2F,4CF_3	0.012	1.9	6.0	9
23	Cl	2F,4CF_3	0.012	2.2	5.7	29
24	Cl	2OMe,4CF_3	0.007	3.0	5.2	58
25a[c]	Cl	2CN,4Me	0.023	0.4	7.2	14
25b[c]	Cl	2CN,4Me	0.117	0.6	6.3	11

[a]IC_{50} value from the human MGAT2 Rapidfire LCMS® assay. [b]Compound is the enantiomerically pure (*S*)-isomer. [c]Compounds are enantiomerically pure but the absolute stereochemistry is unknown.

A graphical overview of the full dataset for this series is shown in Figure 1, of which the compounds described in this paper are a subset. Figure 1A shows permeability plotted against measured $logD_{7.4}$ and trellised according to the 9-substitution pattern. A dashed line showing the value of Caco-2 A-B P_{app} = 10 $x10^{-6}$ cm/s has been added to aid visual comparison. For the compounds with no substitution at the 9-position, only 2/41 (5%) has a P_{app} value > 10 $x10^{-6}$ cm/s. For the 9-methyl set, 12/47 (26%) have a P_{app} value > 10 $x10^{-6}$ cm/s and when only

compounds with a $logD_{7.4}$ > 1.5 are considered, this proportion increases to 12/25 (48%). All of the 15 compounds with a methoxy, ethyl or chloro substituent show P_{app} value > 10 $x10^{-6}$ cm/s, even for those chloro substituted compounds with low lipophilicity ($logD_{7.4}$ 0.5). Figure 1B shows MGAT2 potency plotted against permeability with a target area (pIC_{50} >8; P_{app} > 10 $x10^{-6}$ cm/s shaded in grey). For the un-substituted series only compound of the set of 54 satisfy this criterea. For the 9-methyl compounds, 4/44 (10%) are both potent and permeable. When the 9-OMe/Et/Cl set are considered, 8/15 (53%) achieve the target, highlighting the importance of 9-substitution in achieving potent and permeable compounds in this series.

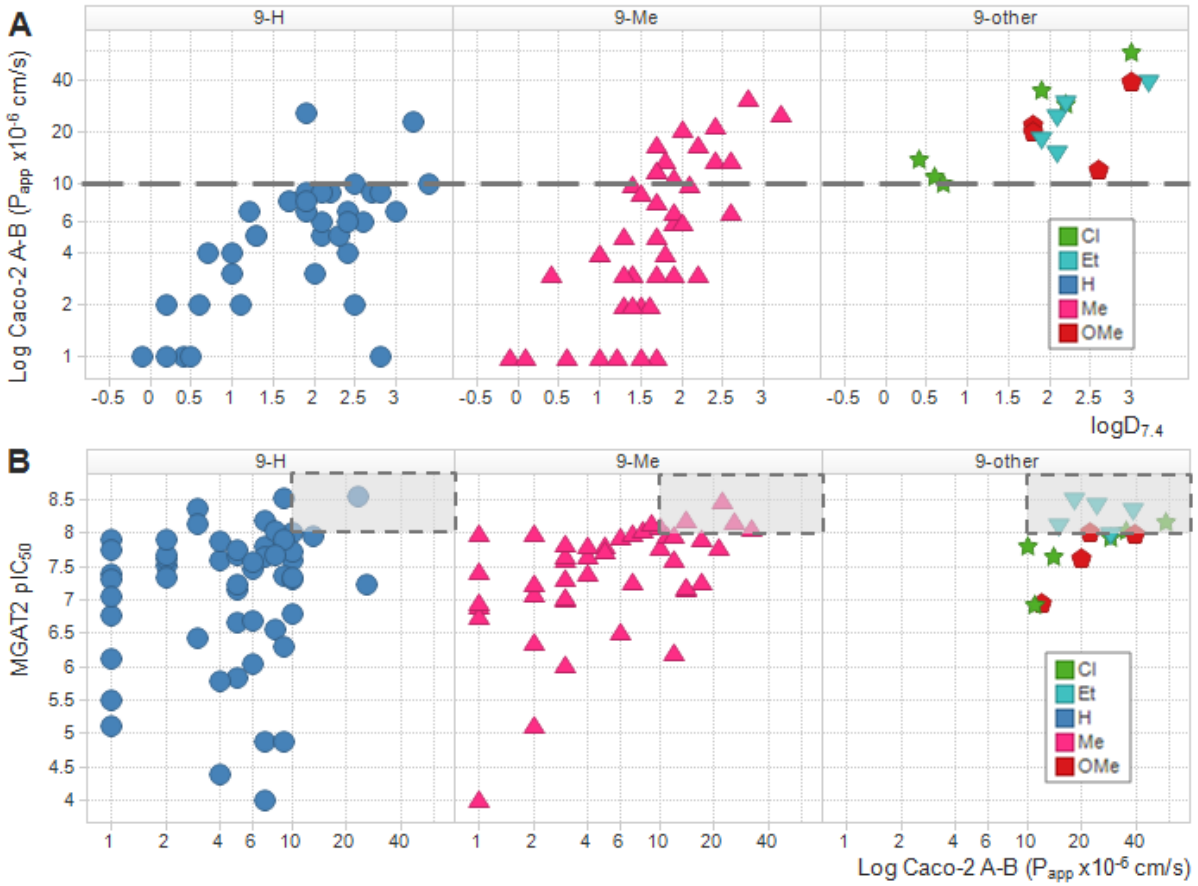

Figure 1. Plots of permeability against $logD_{7.4}$ (A) and MGAT2 potency against permeability (B), grouped by 9-substituent and shaped by 9-substituent.

In an attempt to understand the influence of the 9-substituent on the electronics of the core, the strength of hydrogen-bond donors (logkα) and hydrogen-bond acceptors (logkβ) labelled A-D were calculated using quantum mechanics (Gaussian 09 using B3LYP functional and 6-31G* basis set)[16] and are summarised in Table 5. The labelling and values for the 9-methyl substituted core is shown in the diagram below. Each of the carbonyls has two values corresponding to the orbital lobes on the oxygen lone pairs. These calculations account for both through-bond and through-space electronic effects of the 9-substituent.

Table 5. logkα and logkβ values for 9-substituted compounds

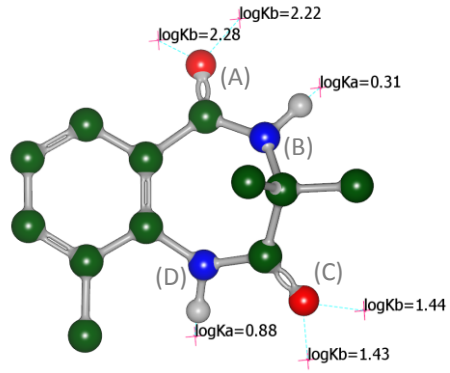

Entry	9-Substituent	Logkβ A	Logkα B	Logkβ C	Logkα D
1	H	2.12/2.12	0.35	1.37/1.38	0.98
2	Me	2.22/2.28	0.31	1.44/1.43	0.88
3	Et	2.25/2.32	0.30	1.48/1.46	0.86
4	Cl	1.88/1.89	0.57	1.22/1.31	0.71
5	CF_3	1.78.1.74	0.68	1.26/1.15	0.83
6	CN	1.45/1.54	0.84	1.08/0.92	1.06

The calculated hydrogen-bond donor and acceptor strengths for a range of 9-substituents corresponding to the compounds from tables 2 and 3 are shown in table 5. These compounds have fixed aryl substitution (2,4-difluoro) and differ only in the substitution of the bis-amide ring (where ethyl or methyl substitution result in equivalent permeability). Simple bivariate statistics were used to elucidate any relationships between Caco-2 P_{app} and calculated hydrogen-bond strength (Caco-2 P_{app} values have been put on a log-scale so as to be normally distributed). The relationship with the strength of the adjacent hydrogen-bond donor (D) clearly shows a strong correlation with log Caco-2 Papp as shown in Figure 2. The probability (P) of this correlation arising by chance is 0.0018, whilst for all other calculated hydrogen-bond strengths $P \geq 0.5$. The correlation of permeability with logkα (D) is also better than for $logD_{7.4}$ (P=0.024). This result helps rationalize the observed permeability: Higher permeability is associated with lower hydrogen-bond donor strength (Cl, CF_3), and low permeability is associated with higher hydrogen-bond donor strength (H, CN).

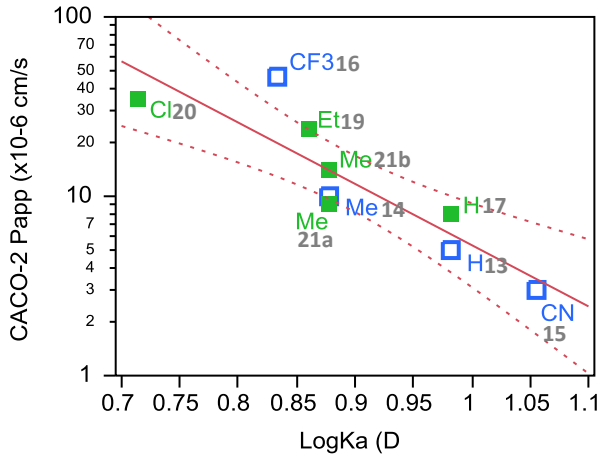

Figure 2. Bivariate plot of Caco-2 P_{app} (log scale) and logkα (D) showing a correlation between the two. Open, blue points are from Table 2; closed, green points are from Table 3. $R^2 = 0.77$; RMSE = 0.46; probability of such a relationship happening by chance is 0.0018.

In order to understand any effects on the solid state of these compounds, small molecule X-ray crystal structures were obtained of several members of this series. Although there are

differences in symmetry and packing density across the un-substituted compounds (**26-28**), similar packing motifs around a strong H-bonded chain between the amides of the cores with a sulphonamide backbone are consistently observed in all three structures (Figure 3). In the 9-chloro analogue (**23**), similar amide interactions between the cores are retained, however, it is noteworthy that the sulphonamide H-bonding motifs are completely absent in this structure (Figure 4).

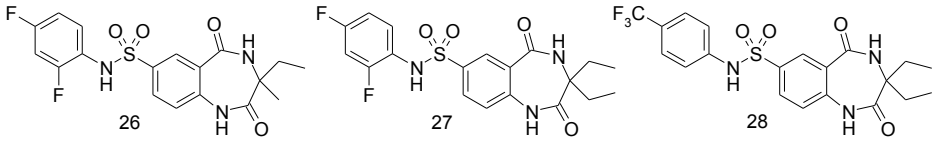

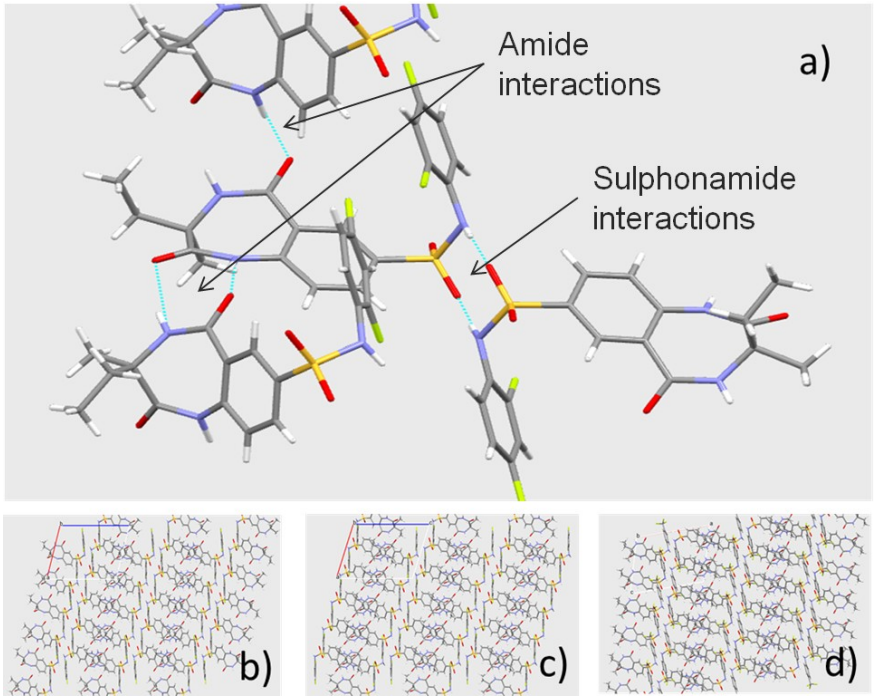

Figure 3. a) Strong H-bonding interactions in **26**. These bonds support a chain structure down the B axis. b) **26** viewed down the B-axis c) **27** viewed down the b-axis d) **28** viewed down the b-axis.

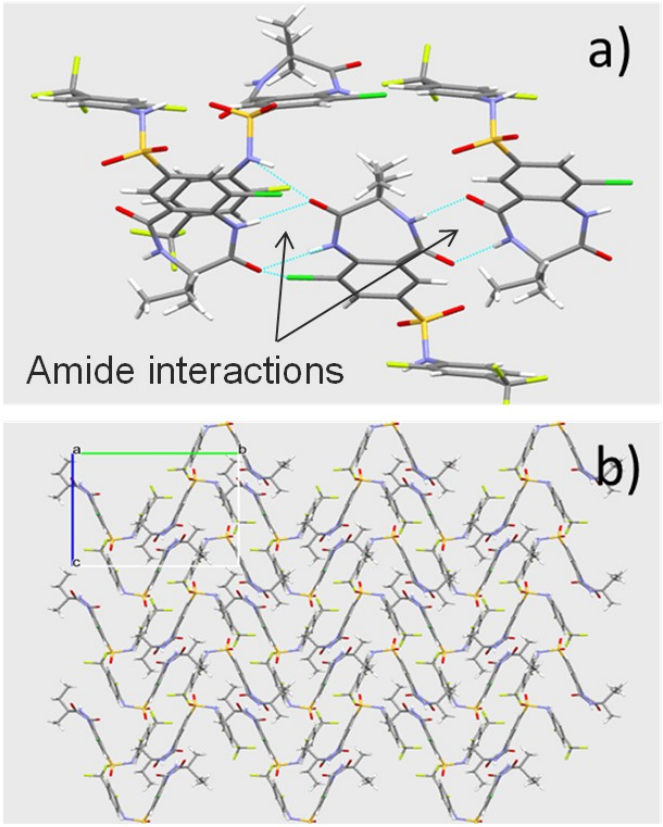

Figure 4. a) Strong H-bonding interactions in **23**. These bonds support a chain structure down the B axis with weaker interactions supporting layering down the a-axis. This is viewed along an intersection of the b/c-axis. b) **23** packing down a-axis.

Compounds were synthesized using a modified version of the previously described route[5] whereby cyclisations were carried out on the amino ester intermediates of type **29** (Scheme 1). This circumvented difficulties associated with isolation of the previously employed amino acids. The amino esters were synthesized from amide coupling of 2-amino benzoic acids **30**, regioselective ring opening of isatoic anhydrides **31** or amide coupling of 2-nitro benzoic acids **32** followed by reduction of the nitro group **33**. Cyclisation to form the core **34** was carried out using acidic conditions and the various substitutions (R6, R8, R9) were generally well tolerated with the exception of (R6 = F) which proceeded in low yield (8%). Acetic acid was initially used in the cyclisation, however, it was noted that acetylation of the aniline was a significant by-product in some cases. This problem was overcome by switching to the more sterically hindered pivalic acid resulting in cleaner reaction profiles and higher isolated yields. Treatment with chlorosulphonic acid generated the corresponding sulphonyl chlorides **35** with excellent regioselectivity for the 7-position regardless of core substitution (R6, R8, R9) in all cases (presumably directed by the aniline amide N1). In the case of R9 = CN, this compound was made from the fully elaborated sulphonamide with R9 = Br and subjected to palladium catalysed cyanation conditions giving compound **15** in good yield.

The enantiomerically pure compounds **17** and **22** (R9 = H) were obtained by chiral HPLC separation of the cyclised core prior to sulphonylation. Treatment with chlorosulphonic acid and sulphonamide coupling gave the desired products with the absolute configuration being identified as (3*S*) based on X-ray crystallography. Compounds **21a** and **21b** (R9 = H) were made in a similar fashion although the absolute configuration was not determined. In the case of compounds **25a** and **25b** these were made by chiral separation of racemic **25** and the absolute configuration was not determined.

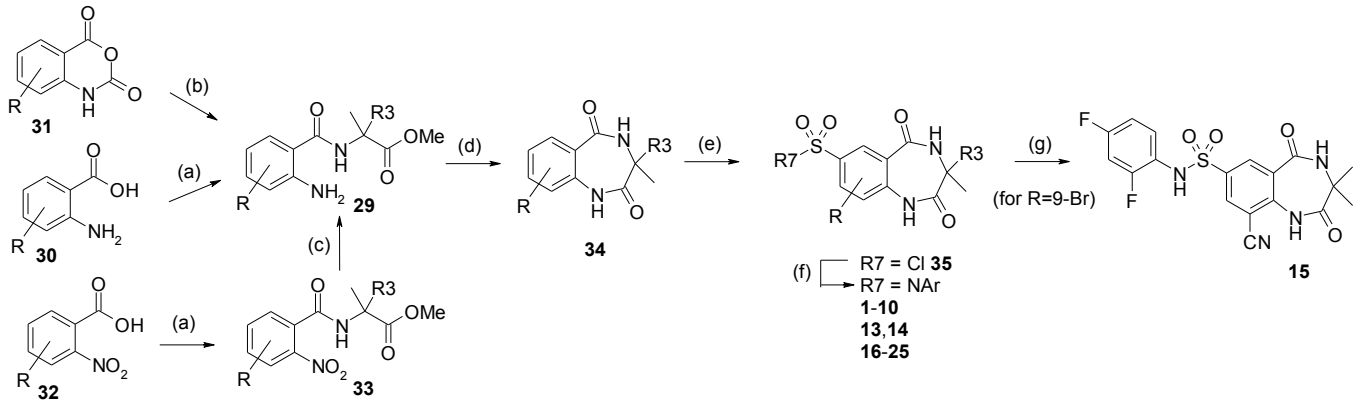

Scheme 1. General synthetic approaches. Reagents: (a) $H_2NCR3(Me)COOMe$, HATU, $(^iPr)_2NEt$, DMF, 76-100%; (b) $H_2NCR3(Me)COOMe$, $(^iPr)_2NEt$, DMF, 60 °C, 55-70%; (c) H_2, Pd/C, EtOH, 93-100%; (d) MeCOOH or ^{t}BuCOOH, μW, 180 - 200 °C, 8-99%; (e) $ClSO_3H$, 65 - 90 °C, 32-100%; (f) $ArNH_2$, pyridine, CH_2Cl_2, 25 - 100 °C, 13-88%; (g) $Pd_2(dba)_3$, XPhos, Zn, $Zn(CN)_2$, DMA, μW, 120 °C, 2 h, 82%

For the aza-analogues it was found that the sulphonylations would not occur on the fully elaborated core (presumably due to the electron deficiency of the pyridyl ring) and so these were made according to the procedures outlined in Scheme 2. For the 8-aza compound **11**, the core was constructed from the 2-chloropyridine **36** *via* amide coupling, Boc deprotection to aniline **38** and cyclisation using pivalic acid to the 8-aza core **39**. The chloro substituent was then displaced with a benzylthiol to give **40** and then oxidized to a sulphonyl chloride and quenched with 4-trifluoromethyl aniline to generate sulphonamide **11**. For the 9-aza compound **12**, an alternative approach was utilized whereby the 2-anilinopyridine **41** was regioselectively converted to the sulphonyl chloride **42** and then coupled in low yield to form the sulphonamide **43**. Amide coupling to form anilinoester **44** and cyclisation under pivalic acid conditions gave sulphonamide **12**.

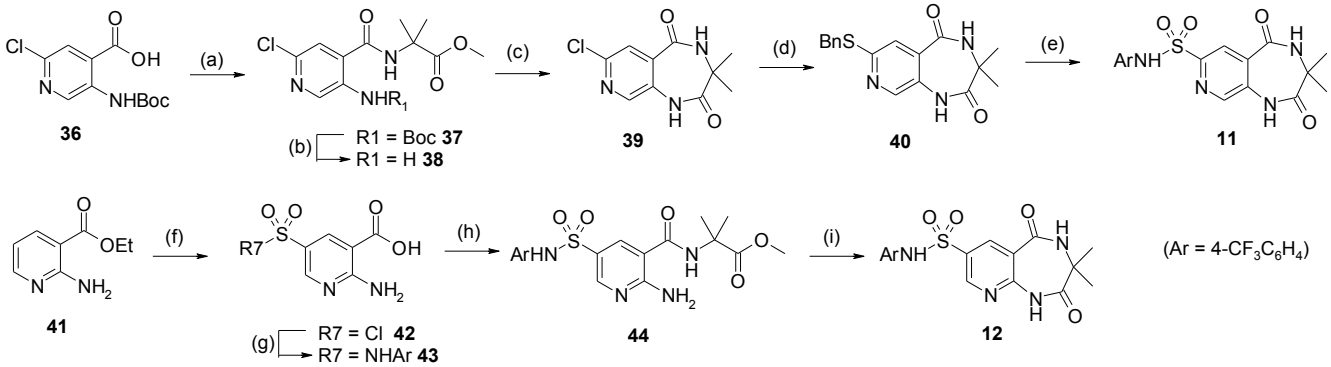

Scheme 2. Synthesis of aza-analogues **11** & **12**. Reagents: (a) $H_2NC(Me_2)COOMe$, HATU, $(^iPr)_2NEt$, DMF, 20 °C, 45 min, 90%; (b) TFA, CH_2Cl_2, 20 °C, 3 h, 100%; (c) ^{t}BuCOOH, μW, 200 °C, 3 h, 35%; (d) BnSH, ^{t}BuOK, DMF, 80 °C, 3 h, 94%; (e) (i) NCS, AcOH, H_2O, 20 °C, 10 min; (ii) 4-$CF_3C_6H_4NH_2$, pyridine, 20 °C, 3 h, 22%; (f) $ClSO_3H$, 65 °C, 18 h; (g) 4-$CF_3C_6H_4NH_2$, pyridine, 20 °C, 3 d, 9% over 2 steps; (h) $H_2NC(Me_2)COOMe$, HATU, $(^iPr)_2NEt$, DMF, 20 °C, 18 h, 29%; (i) ^{t}BuCOOH, 200 °C, 28 h, 56%.

As a representative example of this series, compound **20** was profiled further (Table 6). The compound showed no significant inhibition against four isoforms of the cytochrome P450

enzymes (CYP1A2, CYP2C9, CYP2D6 and CYP3A4 all IC_{50} > 30 μM) and only weak activity against CYP2C19 (IC_{50} 27 μM). No inhibition of the hERG ion channel (IC_{50} >100 μM) was observed. Plasma protein binding showed reasonable free levels (1.7-3.7% free across species) in line with the low lipophilicity of the compound ($logD_{7.4}$ 1.9). The measured pK_a of the sulphonamide NH was 5.9. The aqueous solubility as measured on crystalline material was 150 μM.

Table 6. Physical properties of compound **20**.

Aqueous solubility[a] (μM)	Mouse PPB[b] (% free)	Rat PPB[b] (% free)	Human PPB[b] (% free)	hERG IC_{50} (μM)
150	3.7	3.0	1.7	>100

[a]Solubility of compounds in aqueous phosphate buffer at pH 7.4 after 24 hours at 25 °C (μM). [b]PPB was assessed by equilibrium dialysis in the appropriate species plasma at 37 °C. Free and bound concentrations were quantified by LC-UVMS. [c]Inhibition of hERG channel IC_{50} (μM) in a electrophysiology (IonWorks™) assay.

The oral pharmacokinetic profile of compound **20** was examined in rat at low dose (3 mg/kg) and mouse at high dose (50 mg/kg) with the results are summarised in Table 7. From IV data the compound showed moderate clearance in mouse and low clearance in rat together with a low volume of distribution in both species. Good bioavailabilities (> 60%) were observed in both species.

Table 7. Pharmacokinetic parameters for selected compound **20**[a]

Species	Clp (mL/min/kg)	Vd_{ss} (L/kg)	IV half-life (h)	Oral half-life (h)	Bioavailability (%)
Mouse	29	0.5	0.2	1.2	74
Rat	4.1	0.4	1.3	2.4	69

[a]Dosed PO at 3 mg/kg (rat) and 50 mg/kg (mouse) in suspension (HPMC/Tween) and IV (1 mg/kg) in 5% DMSO: 95% hydroxypropyl β cyclodextrin. Data is mean of two animals in a single experiment.

Conclusion

In summary we have reported the optimization of a series of MGAT2 inhibitors to give potent compounds such as **20** that have favourable physical and pharmacokinetic properties. In particular the permeability, as measured by increased flux in a Caco-2 assay, has been improved through substitution at the 9-position of the core. This was achieved without recourse to increasing the lipophilicity of the compounds but rather through modulation of the hydrogen bond donor strength of an amide NH.

Acknowledgements

Scott Boyd, Ben Chappell, Paul Kemmitt and Paul Schofield are thanked for synthetic contributions. Michael Tonge is acknowledged for generating enzyme inhibition data. Philip MacFaul is thanked for DMPK support and Per Svensson and Anne Ertan for crystallography contributions. We also thank Nicholas Newcombe and Andrew Turnbull for project leadership.

References

1. Yen, C-L. E. and Farese, R. V. Jr. *J. Biol. Chem*. **2003**, *278*, 18532.
2. Bell, R. M. and Coleman, R. A. *Annu. Rev. Biochem*. **1980**, *49*, 459.
3. Yen, C-L. E.; Cheong, M-L.; Grueter C.; Zhou, P.; Moriwaki, J.; Wong, J. S.; Hubbard, B.; Mamour, S.; Farese, R. V. Jr. *Nat. Med*. **2009**, *15*, 442.
4. Nelson, D. W.; Gao, Y.; Spencer, N. M.; Banh, T.; Yen, C-L. E. *J. Lipid Res*. **2011**, *52*, 1723.
5. Barlind, J. G.; Buckett, L. K.; Crosby, S. G.; Davidsson, Ö.; Emtenä, H.; Ertan, A.; Jurva, U.; Lemurell, M.; Nilsson, K.; O'Mahony, G.; Petersson, A. U.; Redzic, A.; Wågberg, F.; Yuan, Z.-Q. *Bioorg. Med. Chem. Lett.,* **2013**, *23,* 2721.
6. Waring, M. J.; *Bioorg. Med. Chem. Lett.,* **2009**, *19*, 2844.
7. Waring, M. J.; *Expert Opin. Drug Discov.,* **2010**, *5*, 235.
8. Hayeshia, R.; Hilgendorf, C.; Artursson, P.; Augustijns, P.; Brodin, B.; Dehertogh, P.; Fisher, K.; Fossati, L.; Hovenkamp, E.; Korjamo, T.; Masungi, C.; Maubon, N.; Mols, R.; Müllertz, A.; Mönkkönen, J.; O'Driscoll, C.; Oppers-Tiemissen, H.M.; Ragnarsson, E. G. B.; Rooseboom, M.; Ungell, A.-L. *Eur. J. Pharm. Sci.,* **2008**, *35*, 383.
9. Increasing permeability through alteration of hydrogen bond strength through addition of proximal groups has been described in the literature. For a recent review see Desai, P. V.; Raub, T. J.; Blanco, M.-J. *Bioorg. Med. Chem. Lett.,* **2012**, *22*, 6540.
10. Cox, C. D.; Breslin, M. J.; Whitman, D. B.; Coleman, P. J.; Garbaccio, R. M.; Fraley, M. E.; Zrada, M. M.; Buser, C. A.; Walsh, E. S.; Hamilton, K.; Lobell, R. B.; Tao, W.; Abrams, M. T.; South, V. J.; Huber, H. E.; Kohl, N. E.; Hartman, G. D. *Bioorg. Med. Chem. Lett.,* **2007**, *17*, 2697.
11. Levesque, J. F.; Bleasby, K.; Chefson, A.; Chen, A.; Dube, D.; Ducharme, Y.; Fournier, P. A.; Gagne, S.; Gallant, M.; Grimm, E.; Hafey, M.; Han, Y.; Houle, R.; Lacombe, P.; Laliberte, S.; MacDonald, D.; Mackay, B.; Papp, R.; Tschirret-Guth, R. *Bioorg. Med. Chem. Lett.,* **2011**, *21*, 5547.
12. Rafi, S. B.; Hearn, B. R.; Vedantham, P.; Jacobson, M. P.; Renslo, A. R. *J. Med. Chem.,* **2012**, *55*, 3163.
13. Leeson, P. D.; Springthorpe, B. *Nature Reviews Drug Discovery,* **2007**, *6*, 881.
14. Other groups such as 9-F (Table 1) and 9-CF_3 (Table 2) showed permeability increases in other sets of matched pairs but were viewed on balance as being less optimal than the Cl. In the case of the F, the permeability rise was less pronounced and the CF_3 added both lipophilicity and molecular weight. The exact matched pairs with 9-Cl were not made as part of this program of work.
15. Structure-Activity-Relationship information from sulphonamide library work revealed that 2,4-disubstitution was a preferred motif in this series and that electron withdrawing substituents (particularly in the 2-position) were favourable for potency.
16. (a) Kenny, P. *J. Chem. Inf. Model.*, **2009**, *49*, 1234; (b) P. W. Kenny, *J. Chem. Soc. , Perkin Trans. 2*, **1994**, 199.